MeV ION IMPLANTATION IN ELECTRONIC MATERIALS*

T. A. TOMBRELLO
Division of Physics, Mathematics, and Astronomy, California Institute of
Technology, Pasadena, CA 91125

ABSTRACT

Using MeV ions for the modification of electronic materials offers a
number of advantages: minimizing surface damage; implantation into com-
pleted devices - for example, through contacts or photoresist layers;
producing controlled radiation damage for flux pinning where the ions pass
completely through the sample and thus do not modify its chemical nature;
and enhancing the electronic excitation of the target material versus
collisional damage, as in adhesion enhancement processes. In all cases,
however, one requires a detailed understanding of the new damage mechanisms
that occur and how they can be modified in a controlled way by annealing.
In this report I shall present examples from a number of our experiments:
resistivity and index of refraction modification in semiconductors; adhesion
enhancement; mixing of multilayer structures; and modification of the
electronic properties of insulators and superconductors.

INTRODUCTION

MeV ion bombardment has yet to find a unique role in the modification
of materials, which is in contrast to the increasingly ubiquitous use of
such ions in analysis by Rutherford backscattering spectrometry (RBS).
Nevertheless, there are many examples of the successful application of MeV
ions; in this paper I shall review some that my group have investigated.
However, one must emphasize at the outset that no claim is made for the
uniqueness of the final results - the cleverness of the inv estigators in
our field has usually made it possible to replicate the effects of such
expensive techniques with those that are much better suited to larger-scale
fabrication.

The most obvious advantages that reside in using MeV ions are their
greater range in materials and the fact that collisional damage occurs
appreciably only near the end of that range. Thus, MeV ion implantation
can be employed in completed structures, where the ions are able to pene-
trate contacts, photoresist and cap layers, etc. The damage that occurs in
the overlying material is usually in the form of isolated point defects,
which are caused by the weak residual collisional damage at high energies
and the dominant electronic excitation energy loss. This sort of damage
can usually be annealed at relatively low energies, which makes it more
likely that the desired modification induced by the implanted atoms is
retained.

Since the characterization of implantation-induced damage and
possible changes in local stoichiometry gives us better insight into the
optimization of the processing, the development of analytical techniques is
an essential part of the effort. Often we do not have in advance a de-
tailed recipe for the implantation fluence and the annealing schedule,
neither do we know with sufficient certainty exactly where the ions end up

or their exact spatial distribution. It usually turns out that developing intuition and analytical skills in any given application is the most diffi- cult and time-consuming part of the work. Thus, in the examples cited here I shall indicate the way analysis is intrinsic to achieving the result.

MATERIALS MODIFICATION

Modification by implantation of foreign atoms

I shall begin with examples that are most closely related to how low- energy ion implantation is used, i.e., introducing a foreign atomic species that changes the characteristics of one or more properties of the original material.

For semiconductors we are usually involved in changing the electronic properties of a part of a more complex structure. This implies a control of the spatial extent of the modification; for implantation the transverse localization is achieved by masking, the depth is controlled by varying the ion's energy. The limitations of the control devolve upon the way the ion loses energy in the material. Fluctuations in the energy loss lead to a spread in the implantation depth that limits how thin a layer can be modified; multiple scattering of the ion limits how narrow a transverse feature can be created. For implantation depths of 1-10 μm for heavy ions these limits are both approximately 500 nm, which is roughly consistent with easily available methods of lithography.

Preliminary to the use of MeV ion implantation in actual applications of III-V device fabrication we devoted considerable effort to understanding the nature of the damage mechanisms and how the defects behaved with tempe- rature. In these studies we used the x-ray rocking curve technique exten- sively - studying quantitatively the induced strain and displaced atom distribution as functions of implantation ion type and fluence, substrate temperature, and annealing schedule [1,2]. The nature of the defects and their depth distribution as functions of these same variables were studied in greater detail using MeV heavy ion channeling and cross-sectional transmission electron microscopy [3,4].

In InP [n-type (100) single crystals] we were able to produce deeply buried 10^6 ohm-cm layers by nitrogen ion implantation (5-8 MeV, corres- ponding to depths of 4-6 μm) followed by a short 20 min. anneal [5]. The implanted fluences (typically 10^{14}-10^{16} cm^{-2}) and depth distribution of the ^{15}N ions were confirmed by nuclear resonant reaction analysis (NRRA) with ^{15}N(p,αγ)^{12}C [3,5]. This technique also allowed us to monitor how the implanted nitrogen behaved under annealing, i.e., it did not diffuse and thus is apparently chemically bound and not just trapped in the radiation damaged region caused by the implantation.

In GaAs we were able to produce similar high resistivity layers by MeV oxygen ion implantation at fluences of approximately 10^{14} cm^{-2} [6]. In this case we applied the technique to the construction of a 10 μm wide GaAs/AlGaAs quantum well laser that had an overall efficiency (light out to electrical power in) of greater than 85%, which was a record efficiency at that time [6]. The effect of the ions was to confine the current flow region by the high resistivity boundary and define the wave guide boundary by the small index of refraction difference produced by the compositional intermixing of the GaAs/AlGaAs layers. Subsequently, another group has been able to exploit this method to making similar lasers with widths down to ~1 μm [7].

Modification by induced damage - without implantation

In order to study in greater detail the processes by which III-V layers of different composition are compositionally intermixed by ions passing completely through them, we bombarded AlAs/GaAs superlattices with 2 MeV oxygen ions [8] - as in the GaAs laser application. We found that even though the damage was caused mainly by the electronic excitation part of the ion's energy loss, there was a strongly enhanced uniform intermixing of the layers after subsequent thermal annealing. In these studies the composition versus depth distribution was profiled using secondary mass spectrometry (SIMS) with 8 keV Cs ions. The mechanism that is suggested from the detailed analysis of the results is Al interdiffusion under thermal annealing which has been stimulated through the recovery of the implantation-induced lattice strain field, the reconstruction and the redistribution of lattice defects, and the annealing of lattice damage [8].

In the "melting" behavior of Abrikosov magnetic flux line lattice in $YBa_2Cu_3O_7$ there is still considerable uncertainty in the role played by the pinning of the lines to crystalline imperfections (grain boundaries, lattice defects, etc.). Clearly, what one really wants to study initially is the nature of the intrinsic lattice melting transition - not one controlled partly by poor material. Since we are not yet able to start with "perfect" crystals, we can only investigate the effect on this phase transition by making the material even less perfect - but in a controlled way. To do this we have started by producing isolated point defects uniformly through the samples (~ 25 μm in diameter) by 5 MeV proton irradiation. Since the protons pass completely through the samples, the effects produced come entirely from the increased number of defects - not from implanted hydrogen [9]. The results of these irradiations is that the superconducting transition temperature is depressed with increasing proton fluence, but that the shape of the boundary of the flux lattice melting transition in the magnetic field versus temperature plane is virtually unchanged. Going beyond the effects of point defects will involve using irradiation with heavier ions; in that case one can reach a situation where there are continuous latent ion tracks that pass through the sample, thereby providing a coherent "defect" that may pin the flux lines even more substantially. This is clearly an excellent example of a not-so-obvious application of MeV irradiation, in which the consequences of flawed material are more easily studied by making it even more flawed (but in an understandable, controlled way).

It has been known for some time that MeV ion irradiation of a thin film-substrate system can significantly improve the film adhesion [10]. The initial explanation of the process was the generation of ion tracks in either film or substrate with compositional intermixing at the interface. This is possible when at least one member of the pair of materials is a dielectric or III-V compound but is unlikely in other cases. A problem arose when adhesion enhancement was discovered for a case where neither material allows ion damage tracks to form [11]. We decided, therefore, to examine the case of Au and Ag layers on Si with the high spatial resolution that is possible with XTEM. What we found was that the thin native oxide layer on the Si played an essential role - it allowed latent ion damage tracks to form, which provided migration paths for film atoms to move to the substrate. This was seen to occur for the case of Au atoms, where there is a strong chemical driving force to form stable Au-Si compounds; for Ag films migration did not occur because of the absence of such compounds [12]. Thus, we see the origin of the enhanced adhesion of Au to Si and the reason it does not occur for Ag; however, one should note that this effect could conceivably be used to produce controlled microscopic "valves" for feeding atoms from film to substrate in other material systems.

Some years ago we found that irradiating amorphous carbon films with low energy (~ 100 keV) heavy ions caused a decrease in the film conductivity, while MeV heavy ion irradiation increased the conductivity – giving a total conductivity range of 10^4 [13]. These data are shown in Figure 1. The supposed origin of the effect was that MeV ions caused microscopic graphitic regions to form, keV ions broke these up into lower conductivity amorphous carbon. Subsequently, we have studied this phenomenon in much greater detail by varying the ion energy and fluence and observing the conductivity versus temperature [14,15].

The picture that has emerged has the following general form. In an extended region (tens of Angstroms) around the MeV ion's path there are many energetic secondary electrons. The existence of this high electron fluence makes it possible to break simultaneously a number of carbon-carbon bonds in a local region; since graphite represents the most stable carbon compound, if enough bonds are broken at **the same time**, a graphite ring can form. Using a model for molecular ion desorption to calculate the probability of graphite ring formation [16], we find that the estimated cross section is in agreement with the low-fluence conductivity change.

If we start with low conductivity amorphous carbon films (i.e., having a low graphite concentration), the low-fluence region has a conductivity versus temperature behavior of $\sigma_0 \exp(-S(\Phi,E)T^{-1/2})$, where Φ and E are the ion fluence and energy, respectively. (See Figure 2.) This is typical of Mott variable-range conduction, in which electrons must tunnel between randomly located, isolated conducting regions [17]. As the number of graphitic regions increases the observed conductivity has an added portion that goes as $\sigma_1 + \sigma_2 T$, where the ratio of σ_1 to σ_2 is that of polycrystalline graphite. This part of the conductivity is caused by the formation of connected chains of graphite rings. The growth of this form of conductivity with ion fluence has the form: $1 - \exp[-(q\Phi)^2]$, which is what one obtains from percolation theory [18]. The coefficient q is related to the cross section for the formation of an individual graphite ring; its value turns out to be exactly what we obtained from the low-fluence behavior of the conductivity and the model of Hedin, et al. In the limit of high fluence the film conductivity has the value and temperature expected from polycrystalline graphite, i.e., when no futher chains can form. Data over the whole range of fluences is given in Figure 3.

In this example we began with the modest expectation of using the effect to make resistors in a controlled way over a wide range of values; what we found in addition was a model system in which to study Mott conductivity and percolation networks where we could use MeV ion irradiation to make continuous adjustments in the number and average spacing of the conducting regions - something that could not easily be done otherwise.

SUMMARY

Although one can hardly be exhaustive in the space/time allocated, I have tried to provide enough variety in the examples to suggest how one can use MeV ion implantation in the modification of materials. Even if these techniques do not find eventual commercial application, in the initial stages of development of an idea they provide useful and efficient tools that can be used to surmount a range of difficulties in the prototyping process.
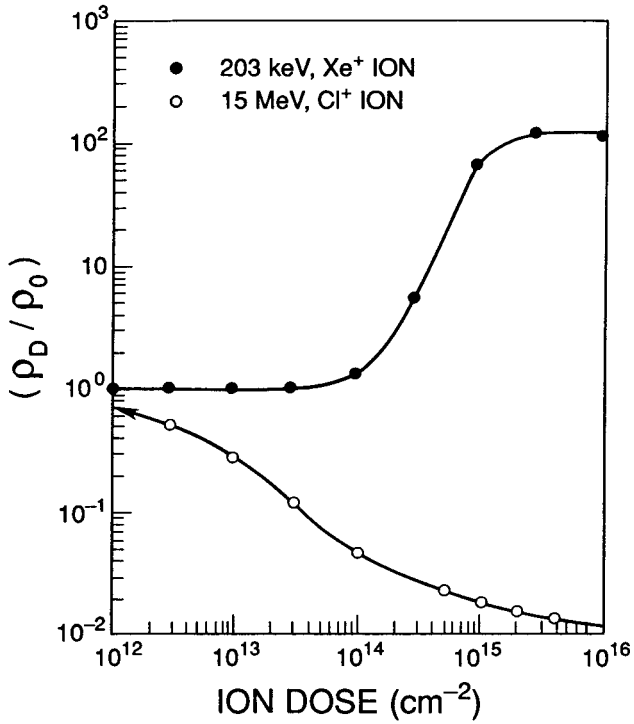
Figure 1: The ratio of the modified resistivity ρ and the pristine resis-
tivity ρ_0 of an evaporated carbon film subjected to low and high
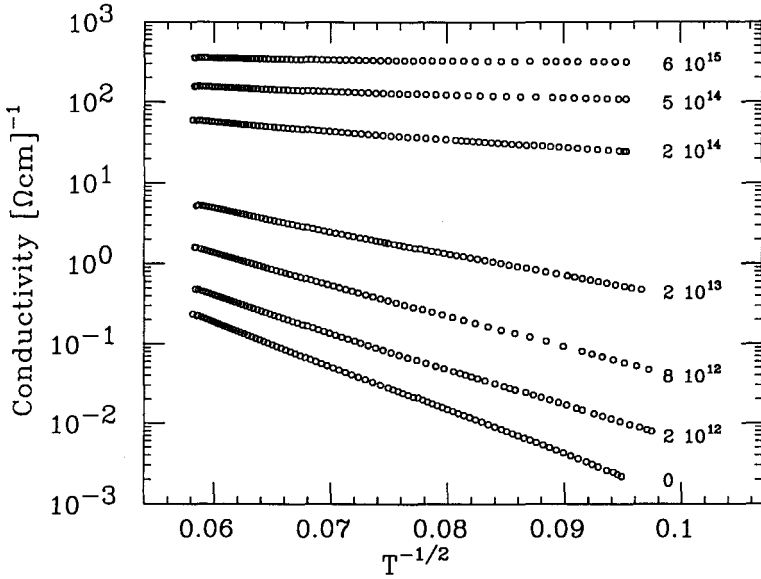energy irradiation, as a function of dose (from ref. [13]).

Figure 2: Selected conductivity versus temperature curves for 15 MeV Cl irradiation. Doses are in ionS per cm^2 (from ref. [15]).
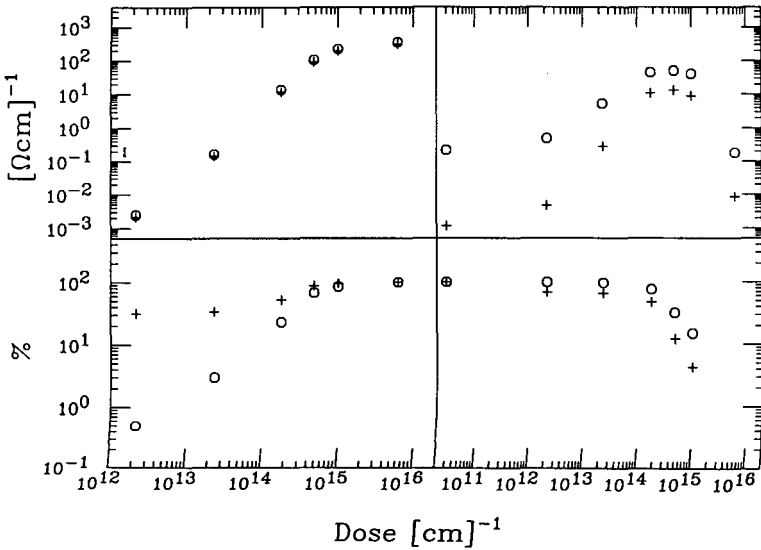

Figure 3: Comparison of graphitic (left) and tunneling (right) contributions to total conductivity of 100 K (crosses) and 293 K (circles). Absolute values (top) and percentages (bottom) (from ref. [15]).

In some of the examples given I have indicated how the use of ion bombardment can provide a way of controlling continuously some of the variables that reflect a material's basic properties. This can give much better intuition about the degree to which particular types of damage are influencing the behavior of that variable. Often one cannot specify the initial value of the damage; by increasing the damage in a controlled way we may learn just how sensitive we are to its presence, i.e., whether our results are compromised from the outset by intrinsic imperfections. As in the case of the ion irradiation of amorphous carbon this control can be used either to provide a wide range of resistivity values or to study the way basic conductivity processes progress as the number of conducting regions increases.

It is quite clear that our use of MeV heavy ion bombardment could be made much more straightforward if there existed a larger body of accumulated data. For example, we definitely need more experimental data on MeV ion ranges and stopping powers, a more accurate way of estimating ion range straggling and multiple scattering, and a better understanding of how damage is produced in some materials by the ion's energy loss in electronic excitation processes (tracks).

As the number of accelerators that can provide MeV ions increases we should expect to find that our exploitation of the technique finds a greater and greater range of application. I hope that this paper will serve to whet your appetite at that prospect.

ACKNOWLEDGEMENTS

REFERENCES

1.   C. R. Wie, T. Vreeland, and T. A. Tombrello, Nucl. Instr. Meth. B16, 44 (1986); Phys. Rev. B33, 4083 (1986); J. Appl. Phys. 59, 3743 (1986).

2.   F. Xiong, C. J. Tsai, T. Vreeland, and T. A. Tombrello, J. Appl. Phys. 69, 2964 (1991).

3.   F. Xiong, C. W. Nieh, T. A. Tombrello, D. N. Jamieson, and T. Vreeland, Vacuum 39, 177 (1989).

4.   T. T. Bardin, T. G. Pronko, F. A. Junga, W. A. Opyd, A. J. Mardinly, F. Xiong, and T. A. Tombrello, Nucl. Instr. Meth. B24/25, 548 (1987).

5.   F. Xiong, T. A. Tombrello, T. R. Chen, H. Wang, Y. H. Zhuang, and A. Yariv, Nucl. Inst. Meth. B39, 487 (1989).

6. F. Xiong, T. A. Tombrello, H. Wang, T. R. Chen. H. Z. Chen, H. Morkoc, and A. Yariv, Appl. Phys. Lett. 54, 730 (1989) and Mat. Res. Soc. Symp. Proc. 144, 367 (1989).

7. R. P. Bryan, J. J. Coleman, L. M. Miller, M. E. Givens, R. S. Averback, and J. L. Klatt, Appl. Phys. Lett. 55, 94 (1989).

8. F. Xiong, T. A. Tombrello, C. L. Schwartz, and S. A. Schwarz, Appl. Phys. Lett. 57, 896 (1990).

9. N.-C. Yeh, D. S. Reed, W. Jiang, U. Kriplani, W. H. Kratel, A. P. Rice, T. A. Tombrello, F. Holzberg, A. Gupta, D. M. Strayer, and A. Kussmaul, Bull. Amer. Phys. Soc. 37, 537 (1992) and paper S 10.39, this meeting.

10. J. E. Griffith, Y. Qiu, and T. A. Tombrello, Nucl. Instr. Meth. 198, 607 (1982).

11. M. H. Mendenhall, Ph.D. Thesis, California Institute of Technology (1983).

12. P. A. Ingemarsson, B. U. R. Sundqvist, C. W. Nieh, and T. A. Tombrello, Appl. Phys. Lett. 54, 1513 (1989).

13. T. Venkatesan, R. P. Livi, T. C. Banwell, T. A. Tombrello, M.-A. Nicolet, R. Hamm, and A. E. Meixner, Mat. Res. Soc. Symp. 45, 189 (1985).

14. T. J. Jones, Ph.D. Thesis, California Institute of Technology (1989).

15. M. Döbeli, T. J. Jones, A. Lee, R. P. Livi, and T. A. Tombrello, Rad. Eff. 118, 325 (1991).

16. A. Hedin, P. Håkansson, B. U. R. Sundqvist, and R. E. Johnson, Phys. Rev. B31, 1780 (1985).

17. N. F. Mott, Conduction in Non-Crystalline Materials, Clarendon Press Oxford, 1987.

18. D. B. Gingold and C. J. Lobb, Phys. Rev. B42, 8220 (1990).